A New Method to Calibrate Shortwave Solar Radiation Measurements

JINHUAN QIU, XIANGAO XIA, JIANGHUI BAI, PUCAI WANG, XUEMEI ZONG, AND DAREN LU

Laboratory for Middle Atmosphere and Global Environment Observation, Institute of Atmospheric Physics, Beijing, China

(Manuscript received 15 May 2013, in final form 3 March 2014)

ABSTRACT

A method is proposed to simultaneously calibrate shortwave (0.3–4 μm) global, direct, and scattering solar irradiance (GSI, DSI, and SSI, respectively) measurements. The method uses the World Radiation Reference (WRR) as a calibration standard and on-site radiation measurements as inputs. Two simple but effective techniques are used in the calibration. The first is to scale SSI and GSI detection sensitivities under overcast skies, which is based on the assumption that SSI should be equal to GSI if DSI is completely scattered and absorbed. The second is a new method to retrieve aerosol optical thickness (AOT), using the ratio of horizontal DSI (HDSI) to GSI measurements under clear and clean conditions. Thereafter, retrieved AOTs are used to drive a radiative transfer model to calculate atmospheric transmittance and then a ratio of GSI to the transmittance. Deviation of this ratio to the WRR is regarded as an indicator of GSI uncertainty, and the calibration transfer coefficient is derived as the WRR ratio. The method is applied to calibrate radiation measurements at Xianghe, China, during 2005. It is estimated from the derived transfer coefficients on 36 clear and clean days that uncertainties of DSI, GSI, and SSI measurements are within −4.0% to 2.9%, −5.9% to 2.4%, and −6.1% to 4.9%, respectively. The calibration is further validated based on comparisons of AOT at 750 nm retrieved from HDSI/GSI to Aerosol Robotic Network (AERONET) AOT products. The maximum deviation between two AOT products is 0.026. The unique advantage of this method lies in its potential applications in correcting historic radiation measurements and monitoring radiometer performance.

1. Introduction

Surface solar radiation is an important factor determining the thermal conditions and the circulation of the atmosphere. Accurate measurement of surface solar radiation is essential for understanding the present climate and potential climatic changes. There are a large number of solar radiation observation sites across the world for measuring shortwave global, direct, and scattering irradiances (GSI, DSI and SSI, respectively) using pyranometers and pyrheliometers. Observations began in the 1880s (Roosen et al. 1973; Stothers 1996). The Global Energy Balance Archive (GEBA) produces quality-controlled monthly datasets of surface energy fluxes, which are available on the Internet stretching back to October 1997 (Gilgen and Ohmura 1999). To provide surface solar radiation for validating satellite retrievals and model simulations, as well as monitor long-term changes in surface irradiance, the World Meteorological Organization/International Council of Scientific (WMO/ICSU) Joint Scientific Committee for the World Climate Research Programme (WCRP) proposed in October 1988 the establishment of an international Baseline Surface Radiation Network (BSRN) (Ohmura et al. 1998). The on-site pyranometer and pyrheliometer are usually calibrated once every one or two years through a calibration transfer process, in which they are compared with world or national standard instruments to determine their calibration coefficients. There are some uncertainties associated with field solar radiometer measurements caused by instrument stability, detector contamination, temperature effects, and so on (Dutton et al. 2001; Ji and Tsay 2010). For example, one would expect a significant influence of heavy aerosol loading on solar radiometer measurements in China if the detector dome is not cleaned very often. Therefore, a reliable method to monitor radiometer performance is highly desirable. Such a method would also be very useful for evaluating the data quality of historical solar radiation measurements.

Corresponding author address: Jinhuan Qiu, Institute of Atmospheric Physics, Chinese Academy of Sciences, Hua Yan Bei Li, Chao Yang District, Beijing 100029, China.
E-mail: jhqiu@mail.iap.ac.cn

DOI: 10.1175/JTECH-D-13-00114.1

Based on the fact that GSI is weakly sensitive to aerosol optical parameters in the case of aerosol optical thickness (AOT) < 0.2, Qiu et al. (2008) presented a method to estimate the uncertainties of historic GSI data in China. This evaluation method is not completely independent of DSI data quality, so further study on this issue is still required. More specifically, we need a simple yet effective calibration method that, as far as possible, is independent of radiation data quality. We developed a new method to fulfill this goal. One of the features of this method is that we can calibrate DSI, GSI, and SSI simultaneously. The method directly takes the World Radiation Reference (WRR) as the calibration standard and uses on-site radiation measurements as inputs. It does not assume a priori accuracy of any DSI, GSI, and SSI measurements using the following two key techniques. The first is to scale SSI and GSI detection sensitivities under overcast conditions. The assumption behind this step is that SSI and GSI measurements should be equal to each other if DSI is completely scattered and absorbed. The function of this step is to obtain a good estimation of SSI/GSI and thereby the ratio of the horizontal DSI (HDSI) to GSI. The HDSI is defined to be the difference between GSI and SSI. The second is to retrieve AOT from HDSI/GSI. The reason for the retrieval of AOT using HDSI/GSI is that this ratio is very sensitive to AOT, but not too sensitive to aerosol optical properties, such as single scattering albedo (SSA) and scattering phase function. The retrieved AOT is then used to drive a radiative transfer model (RTM) to calculate atmospheric transmittance, and then finally solar radiometers are calibrated.

The paper is organized as follows. An introduction to the method is presented in the following section. Section 3 presents an application and evaluation of this new calibration method. The conclusions of the study are presented in section 4.

2. Method

The calibration method is introduced as follows: first, the principle and calibration formula used in the two key techniques are explained; second, the criteria used for the selection of radiation data in the calibration are described; and finally, the calibration processes are presented.

a. The principle and calibration formula

The ground-based shortwave GSI, free of uncertainties (E_{GSI}, in units of $\mathrm{W\,m^{-2}}$) is represented as follows:

$$E_{\mathrm{GSI}} = \eta_{\mathrm{Tot}} E_{0,\mathrm{SW}}, \tag{1}$$

where $E_{0,\mathrm{SW}}$ is the integration value ($1338.66\,\mathrm{W\,m^{-2}}$) of solar spectral intensity (0.3–4 μm) at the top of the atmosphere (TOA), which is taken from the final report of the eighth session (WMO 1982), and treated as the WRR; and η_{Tot} is the shortwave total atmospheric transmittance. It should be noted that the two sides of the equation may not be equal to each other due to the likely improper calibration of the pyranometer. Therefore, the E_{GSI} data should be corrected using a calibration transfer coefficient (f_{GSI}) when η_{Tot} is determined as accurately as possible, that is,

$$f_{\mathrm{GSI}} E_{\mathrm{GSI}} = \eta_{\mathrm{Tot}} E_{0,\mathrm{SW}}. \tag{2}$$

Then, we have

$$f_{\mathrm{GSI}} = \eta_{\mathrm{Tot}} E_{0,\mathrm{SW}} / E_{\mathrm{GSI}} = E_{0,\mathrm{SW}} / E_{0,\mathrm{GSI}}; \tag{3}$$

$$E_{0,\mathrm{GSI}} = E_{\mathrm{GSI}} / \eta_{\mathrm{Tot}}. \tag{4}$$

At the TOA $E_{0,\mathrm{GSI}}$ is the retrieved solar irradiance from a ground-based GSI measurement. If $E_{0,\mathrm{GSI}} > E_{0,\mathrm{SW}}$ (WRR), then $f_{\mathrm{GSI}} < 1$ and vice versa. We can see that the accurate derivation of f_{GSI} depends upon the uncertainty in η_{Tot}. Therefore, the question arises as to how to determine η_{Tot} as accurately as possible. This might be achieved under the condition that η_{Tot} is weakly sensitive to the atmospheric parameters. Cloudy conditions should be avoided because cloud optical properties are not easily derived and modeled. Aerosol and water vapor are the most variable factors impacting η_{Tot} under cloud-free skies. If water vapor measurements are available, then AOT is the most important factor determining η_{Tot}. Aerosol optical properties, such as aerosol SSA and asymmetry factors, exert only a marginal effect on η_{Tot} if AOT < 0.2. Therefore, we can use an RTM to calculate η_{Tot} effectively if AOT can be retrieved from the solar radiation measurements. DSI is very sensitive to AOT, and so it is widely used to retrieve AOT (Eck et al. 2005; Qiu 1998). However, AOT may be poorly retrieved if the DSI measurements are not properly calibrated. Obviously, it is not suitable to directly use noncalibrated DSI in AOT retrievals, so a new approach is required in order to retrieve AOT from noncalibrated measurements. Here, we propose a method to fulfill this goal, in which the ratio of HDSI to GSI (R_f) is used for AOT retrievals:

$$R_f = \frac{\mathrm{HDSI}}{\mathrm{GSI}} = 1 - \frac{\mathrm{SSI}}{\mathrm{GSI}} = 1 - \beta_R. \tag{5}$$

One of the most important advantages of using R_f for AOT retrievals is that we can derive a good estimation of β_R under overcast conditions, and thereby a priori absolute calibrations of GSI and SSI are not required.

Furthermore, in the case of a small ratio of AOT to the cosine of the solar zenith angle (μ_0), there are three additional advantages if R_f is used to retrieve AOT. First, R_f is weakly sensitive to SSA. This is because of the weaker sensitivity of HDSI to SSA and its dominant contributor to GSI. Second, R_f is very sensitive to AOT, being equivalent to HDSI, because GSI varies very smoothly with AOT. Third, R_f is not sensitive to the surface albedo due to a weak dependence of GSI on the surface albedo if AOT < 0.2 (Qiu et al. 2008). Note that GSI and SSI are usually measured by two independent pyranometers, so quite different performances of these two pyranometers will undoubtedly lead to large uncertainties in the derivation of β_R if we use the measurements directly. So, the question arises as to how to determine β_R as accurately as possible. DSI is expected to be completely scattered and absorbed if the sky is covered by thick stratus clouds, and thereby SSI should be equal to GSI in such a case. Therefore, we can adjust the sensitivities of the two pyranometers to the same scale based on the aforementioned assumption. Hereafter, this scale is used to estimate β_R under cloud-free and clean conditions (AOT < 0.2).

The AOT, retrieved from R_f, is used in calculating direct shortwave transmittance η_{Dir}. Then, similar to f_{GSI} determination according to Eqs. (2) and (3), the DSI calibration transfer coefficient f_{DSI} is determined according to the following equations:

$$f_{\mathrm{DSI}} E_{\mathrm{DSI}} = \eta_{\mathrm{Dir}} E_{0,\mathrm{SW}}; \tag{6}$$

$$E_{0,\mathrm{DSI}} = E_{\mathrm{DSI}} / \eta_{\mathrm{Dir}}. \tag{7}$$

Since the sensitivities of SSI and GSI measurements are relatively scaled, the GSI calibration transfer coefficient f_{GSI} is used to yield the SSI calibration transfer coefficient f_{SSI} as follows:

$$f_{\mathrm{SSI}} = f_{\mathrm{GSI}} / f_{\mathrm{Scaling}}, \tag{8}$$

where f_{Scaling} is the sensitivity scaling factor, that is, the measured ratio of β_R under overcast conditions. Then, based on the scaling, Eq. (5) can be changed as follows:

$$R_f = 1 - \frac{\mathrm{SSI} \times f_{\mathrm{Scaling}}}{\mathrm{GSI}}. \tag{9}$$

b. *Criteria for the selection of radiation data in the calibration*

As analyzed above, solar radiation data in the case of a smaller AOT and a larger μ_0 are suitable for the calibration. Based on the dependence of β_R on AOT and μ_0, β_R is used as a key selection criterion in this paper as a result of the following considerations. First, β_R can be directly determined from measured GSI and SSI data. Second, as shown in Fig. 1, β_R decreases as AOT decreases or μ_0 increases, and so the calibration accuracy should be improved by selecting solar radiation data with smaller β_R.

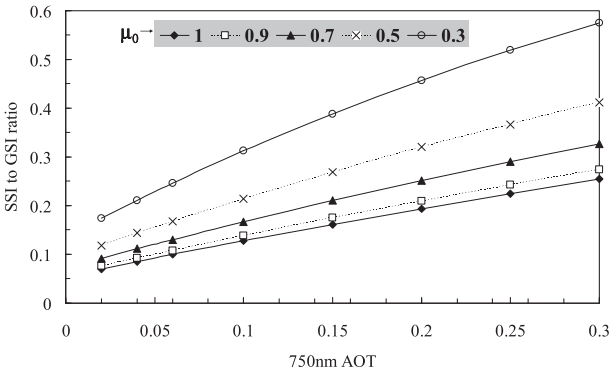

FIG. 1. SSI-to-GSI ratio (β_R) vs 750-nm AOT for an AWE of 1.0 and different μ_0.

Selecting smaller β_R in the calibration will produce smaller calibration uncertainty; however, the calibration samples are expected to decrease. Therefore, we use 0.2 (β_R) as the criterion in the application to meet these two requirements. Furthermore, daily variation of the calibration coefficients should vary little, so an extra criterion is also used, that is, the root-mean-square (RMS) deviation of daily transfer coefficients should be <1%.

c. *Major calibration processes*

An important part of the calibration is the AOT retrieval from R_f. As analyzed above, radiation measurements with $\beta_R < 0.2$ ($1 - \beta_R$ = HDSI/GSI > 0.8) are used in the calibration, implying a more than 80% contribution of HDSI to GSI. Given the fact that GSI varies smoothly with AOT, the AOT retrieval from R_f is principally based on the DSI characteristic. DSI is mostly determined by the wavelength-dependent AOT, and so a key problem in using DSI for the AOT retrieval is the effect of aerosol size distribution (ASD) uncertainty. Approximately one-half of solar radiation at the TOA is within the wavelength range of <732 nm (WMO 1982). It has been pointed out that the wavelength corresponding to one-half of DSI on the ground is approximately 750 nm for different AOTs. The AOT at 750 nm can be retrieved with an accuracy of better than 5% if a power-law ASD with an Ångström wavelength exponent (AWE) of 1.0 is used (Qiu 1998). Therefore, R_f is used to retrieve AOT at 750 nm, in which an AWE of 1.0 is used. Using the AWE and the 750-nm AOT, AOTs in the whole shortwave spectrum are determined and then used in the RTM calculations.

In summary, the calibration algorithm consists of the following steps:

1) Determine the sensitivity scaling factor, f_{Scaling}, using SSI and GSI data in the case of DSI = 0.
2) Use SSI and GSI data with $\beta_R < 0.2$ as well as the last step's f_{Scaling} to determine the measured R_f according to Eq. (9).
3) Use R_f and an AWE of 1.0 to retrieve the AOT at 750 nm. Different AOTs at 750 nm are inputted into the RTM to calculate the DSI, GSI, and then R_f. The AOT is regarded as the retrieval if the RTM-calculated R_f from it is equal to the measured R_f.
4) Use the RTM with the AOT retrieval from step 3 to calculate the transmittances η_{GSI} and η_{DSI}.
5) Use η_{GSI} and η_{DSI} to determine the transfer coefficients: f_{GSI}, f_{DSI}, and f_{SSI}.
6) Select calibrations according to the above-mentioned criteria.

It should be emphasized that the "calculated" R_f in the AOT retrieval represents the ratio of the RTM calculations of HDSI and GSI, and the "measured" R_f is determined from measurements of SSI and GSI. The eight-stream Discrete Ordinate Radiative Transfer model (DISORT) algorithm with the horizontally uniform assumption (Stamnes et al. 1988) is used in this study. The main input parameters for the η_{GSI} calculation include 1) AOT; 2) AWE (or ASD); 3) aerosol refractive index; 4) column water vapor amount; and 5) surface albedo. The AOT is the parameter to be retrieved. The AWE and refractive index are used to calculate the aerosol scattering phase function and SSA.

3. Application and evaluation

a. Site and measurements

The new calibration method is applied to the measurements of surface solar radiation during 2005 at Xianghe, China, one of the BSRN sites and Aerosol Robotic Network (AERONET) sites (Holben et al. 1998). Kipp–Zonen CM21 radiometers are used to measure the GSI. The GSI can also be derived by summing the direct and diffuse components of radiation, which are measured separately by an Eppley Normal Incidence Pyrheliometer (NIP) and a black-and-white radiometer (B&W), both mounted on an EKO STR-22 solar tracker (Xia et al. 2007). The radiometers take samples every second, but 1-min means and standard deviations are saved to a Campbell datalogger. A redundant set of broadband radiometers is used to ensure the precision of measurements and to rule out possible biases by physical problems (e.g., misaligned solar shadowing disk). The data are quality checked using the BSRN quality control procedures (Ohmura et al. 1998) and submitted to the BSRN archive. It is estimated that the field measurement uncertainties are 3%, 6%, and 6% for direct, diffuse, and global measurements, respectively, using NIP and B&W radiometers (Stoffel 2005).

AOTs at seven wavelengths (340, 380, 440, 500, 670, 870, and 1020 nm) are derived with an uncertainty of 0.01–0.02 from Cimel Electronique sun-photometer measurements (Eck et al. 1999). The measurements at 940 nm are used for the derivation of the column water vapor amount. Aerosol size distribution, the refractive index, and SSA are retrieved from the sky radiance measurements and AOTs (Dubovik and King 2000; Eck et al. 2005). The data used here are level 2.0 quality-assured data that have been prefield and postfield calibrated, automatically cloud screened (Smirnov et al. 2000), and manually inspected. If AERONET water vapor data are not available, then we can use operational meteorological observations of surface water vapor pressure to derive them (Yang and Qiu 2002).

Comparisons of AOT retrievals by the present R_f method and the broadband extinction method (BEM) (Qiu 1998, 2003) with AERONET data are treated as an independent indicator of the calibration accuracy. In the RTM calculation for the AOT retrievals and radiometer calibrations, the aerosol AWE is set to 1 and the aerosol refractive index is $1.5–0.01i$, which is close to the mean AERONET values (Xia et al. 2006). The surface albedo (SA) is taken from the monthly-mean MOD43 product (Schaaf et al. 2002). GSI is very weakly sensitive to the SA variation if AOT is less than 0.2 (Qiu et al. 2008). One would expect a negligible effect of SA uncertainty on radiation calibrations.

b. Radiation calibrations

A modified cloud-screening method is used for detecting clear skies from surface solar radiation measurements (Xia et al. 2006). Furthermore, we use two additional criteria to select radiation measurements in the calibration. The first and also most essential criterion is that β_R should be less than 0.2. The second is that the RMS deviation among calibration transfer coefficients in one particular day should be lower than 1%. There are a total of 36 clear and clean days during 2005 at Xianghe meeting the requirements for the calibration.

As pointed out in the last section, the calibration requires the scaling of SSI and GSI detection sensitivities under overcast skies. To weaken the effect of radiation measurement noises on the scaling, only the SSI and GSI data that are larger than $100\,\text{W}\,\text{m}^{-2}$ and measured on overcast days with DSI $< 1\,\text{W}\,\text{m}^{-2}$ are selected in the scaling.

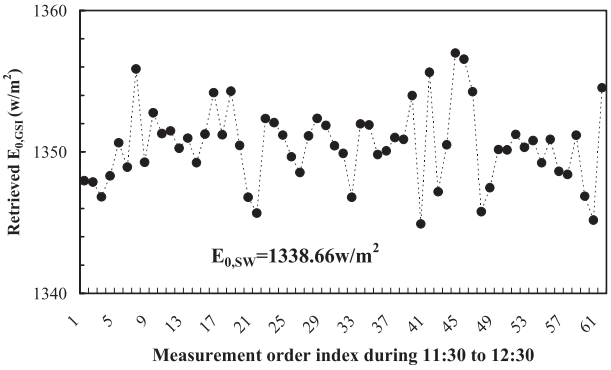

FIG. 2. Sixty-one sets of $E_{0,GSI}$ retrieved from the GSI data during 1130–1230 LT 12 Jan 2005.

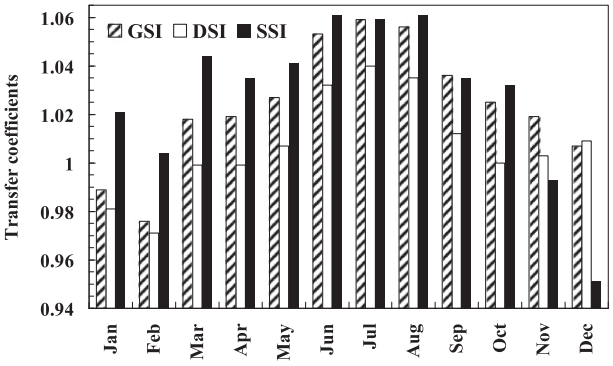

FIG. 3. Monthly-mean transfer coefficients of GSI, DSI, and SSI.

As mentioned earlier, solar radiation data associated with large μ_0 are more suitable for the calibration. So, 61 radiation data points at around midday, local time (1130–1230 LT) are used. Figure 2 shows the $E_{0,GSI}$ estimation on 12 January 2005. The relative deviation of the mean $E_{0,GSI}$ from the WRR $E_{0,SW}$ is 0.88%. There is a very small difference among the 61 $E_{0,GSI}$ retrievals, with an RMS deviation of 0.20%. The maximum deviation of individual $E_{0,GSI}$ to the mean $E_{0,GSI}$ is 0.48%.

Figure 3 shows the monthly-mean transfer coefficients of GSI, DSI, and SSI. The monthly mean is calculated from calibrations on more than 3 days in each month. It is not surprising that the transfer coefficients for the GSI, DSI, and SSI in summer are larger than those in winter, which is likely caused by lower instrument sensitivity when the temperature is high (Coulson 1975). Temperature affects CM21 accuracy by 2%–3%, and instrumental uncertainty can be reduced to below 1% following correction of the temperature effect (Ji and Tsay 2010; Ji et al. 2011). The mean nighttime offset of the CM21 radiometer used in this study—an indicator of the magnitude of the infrared loss in global measurements—is about $-2\,\mathrm{W\,m^{-2}}$ (Xia et al. 2007), which is corrected using the method suggested by Dutton et al. (2001). Monthly-mean transfer coefficients of GSI, DSI, and SSI change between 0.98 and 1.06, 0.97, and 1.04, and 0.95 and 1.06, implying their uncertainties vary between −5.9% and 2.4%, −4.0% and 2.9%, and −6.1% and 4.9%, respectively. The estimations are in good agreement with the measurement uncertainties of 3%, 6%, and 6% for DSI, GSI, and SSI, respectively, as suggested by Stoffel (2005). The annual mean transfer coefficients of GSI, DSI, and SSI are 1.02, 1.01, and 1.03, respectively.

c. *Comparisons of AOT between BEM retrievals and AERONET products*

AOT data used in comparisons should meet the following four requirements: 1) the measurement time difference between our retrieval and AERONET should be less than 30 s; 2) $\mu_0 > 0.3$; 3) AERONET AOT < 3.0; and 4) there should be at least five AOTs in one day.

Two kinds of AOT at 750-nm retrievals are used to compare with AERONET AOTs. The first consists of retrievals based on the R_f data for days when calibration is applied. The second consists of retrievals based on the BEM algorithm (Qiu 1998; 2003) using original or recalibrated HDSI (GSI minus SSI) data. The AOT at 750 nm for AERONET is derived from the AOT at 670 nm and the AWE.

Figure 4 compares the AOT retrievals from R_f at 36 days with corresponding AERONET AOTs during the period 1130–1230 LT. Note that the AOT retrievals and radiation calibrations are simultaneously performed, which does not require a priori calibration of radiation data. There is very good agreement between AOTs from our retrievals and AERONET. Among the 36 days of AOT comparisons, the maximum deviation is 0.026 and the RMS deviation is 0.008. Clearly, the good agreement between our AOT retrievals with AERONET AOT products indicates a good performance of the new calibration method.

Figure 5 compares BEM AOTs from the original and recalibrated HDSI with AERONET AOTs. The monthly-mean transfer coefficients (see Fig. 3) are used to recalibrate GSI and SSI data and then to retrieve AOT. There are a total of 234 days with BEM AOT retrievals. A good agreement between AOTs from BEM and AERONET is obtained. The deviation of monthly-mean BEM AOTs using the original HSDI data from AERONET AOTs varies from −0.048 to 0.044. The deviations using recalibrated HSDI varies from −0.029 to 0.029, which is about one-half of the former values. The RMS deviations of BEM AOTs from the original and recalibrated HDSI are 0.030 and 0.016, respectively, and the annual mean deviations are 0.012 and −0.001, respectively. It is clear that better retrievals of AOT are

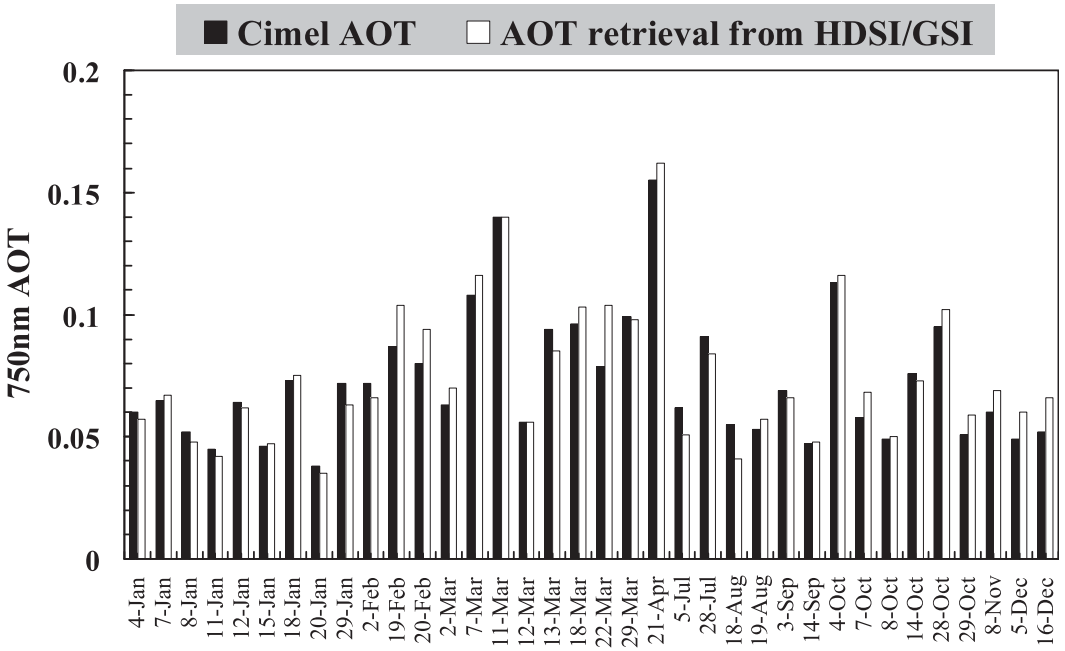

FIG. 4. Comparison of AOT retrievals from the new method based on HDSI/GSI with AERONET AOTs.

obtained from recalibrated HDSI data, as compared with that from original HDSI data.

d. Effect of uncertainties in the AWE and aerosol imaginary index

Note that in the RTM calculation for the AOT retrievals and calibrations, the AWE is set to 1 and the aerosol imaginary index (AII) is set to 0.01 in the RTM calculations. The uncertainties associated with these parameters are the two most essential error sources in the calibration. If the AWE is set to 0.5 or 1.5 instead of 1.0, then the RMS deviations of the GSI and DSI calibration coefficients in those 36 days (compared with those using 1.0) are within 1.03% and 1.17%, respectively. If the AII is set 0.005 or 0.015 instead of 0.01, then the RMS deviations of the GSI and DSI calibration coefficients are 1.14% and 1.22%, respectively. Therefore, the calibration uncertainty is estimated to be less than 2%, caused by a $\pm 0.5/\pm 0.005$ deviation in AWE/AII values. It should be noted that the smaller the AOT is, the smaller the uncertainty is of the AOT retrieval by the BEM, as caused by the AWE uncertainty (Qiu 1998, 2001). Therefore, as shown in Fig. 6, a better calibration accuracy is achieved in cases of smaller AOT. Figure 6 compares deviations of GSI transfer coefficients using AWEs of 0.0, 0.5, 1.5, and 2.0 with that using an AWE of 1.0 on 2 particular days (18 August and 21 April). The AERONET

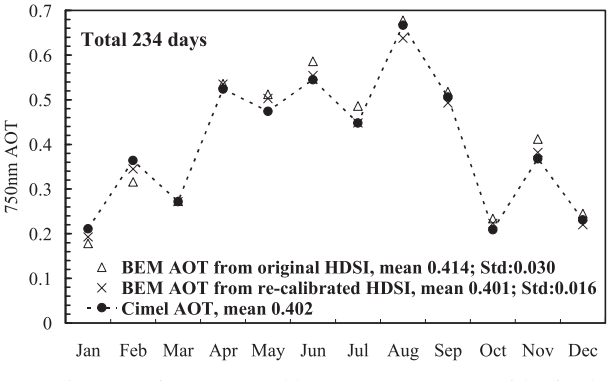

FIG. 5. Comparisons of monthly-mean BEM AOTs with Cimel Electronique AOTs.

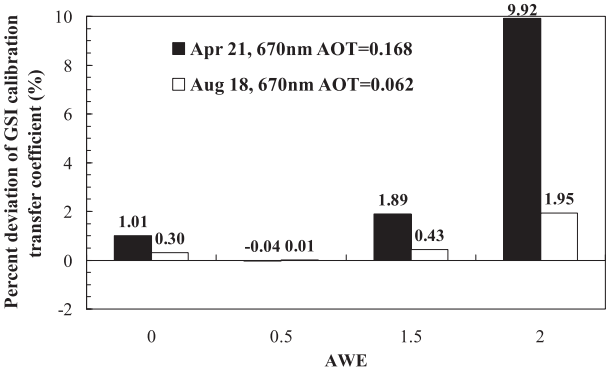

FIG. 6. Deviations of GSI calibration transfer coefficients using AWEs of 0.0, 0.5, 1.5, and 2.0 with the coefficient using an AWE of 1.0.

670-nm AOTs on those 2 days are 0.062 and 0.168, and their AWEs are 1.134 and 0.715, respectively. When the AWE changes from 0.0 to 1.5, the GSI transfer coefficient deviations are within ±0.43% for 18 August and ±1.89% for 21 April. The deviations evidently increase when an AWE of 2.0 is set, being 1.95% and 9.92% for 18 August and 21 April, respectively. The uncertainty in the larger AOT case (21 April) is much larger. Furthermore, the DSI transfer coefficient deviations are almost the same as the GSI ones, being within ±0.46% and ±1.98% for 18 August and 21 April, respectively, when the AWE changes from 0% to 1.5%, and from 1.91% to 10.2%, respectively, when an AWE of 2.0 is set. In addition, we find that the transfer coefficient deviation, caused by the AII uncertainty, also increases with increasing AOT. The deviations are within ±0.65% for both the GSI and DSI calibrations when AIIs of 0, 0.005, 0.015, and 0.02 are set instead of 0.01 in the 0.062 AOT case (18 August), and they raise to within the range ±2.16% in the 0.168 AOT case (21 April). The above deviation is an analysis of the GSI and DSI transfer coefficient uncertainties for the suburban aerosol type over a site at Xianghe, near Beijing, based on an assumed AWE of 1.0 and an AII of 0.01. On the basis of the analysis, we now estimate the uncertainties caused by these assumptions for different aerosol types.

Using AERONET data, Dubovik et al. (2002) studied the variability of absorption and optical properties of key aerosol types observed at a number of locations throughout the world. The study indicated that AII changes between 0 and 0.02, except for biomass-burning aerosol over the African savanna in Zambia, where AII is within 0.021 ± 0.004. As analyzed above, when AIIs ranging from 0 to 0.02 are set instead of 0.01, the GSI and DSI transfer coefficient deviations are within ±0.65% for the case of the below 0.062 AOT at the 670-nm wavelength (18 August), or ±2.16% for 0.168 (21 April). Therefore, if radiation measurements in below 0.062 (or 0.168) AOT conditions are used in the calibrations, then a below 1% (or below 2%) uncertainty, caused by assuming an AII of 0.01, can be achieved for a wide variety of aerosol types, except for biomass-burning aerosol. As also analyzed by Dubovik et al. (2002), the AWE ranges from −0.1 to 2.5 for worldwide aerosol types. Larger AWEs (1.2–2.5) are found for urban–industrial and mixed aerosol over National Aeronautics and Space Administration (NASA)'s Goddard Space Flight Center (GSFC) in Greenbelt, Maryland, and much lower AWEs (<0.9) for desert and oceanic aerosol over Solar Village, Saudi Arabia. The AOT over GSFC is often very small. According to AERONET data at GSFC in 2005, there are a total of 73 days with below 0.062 AOT conditions at the 670-nm wavelength. The mean 750-nm AOT on these 73 days is 0.034, and the mean AWE is 1.686. The smaller the AOT is, the weaker the effect of AWE uncertainty on the radiation calibrations. If the radiation measurements on the 73 days are used, then a below −2% calibration uncertainty is estimated when an AWE of 1.0 is inputted. In the case of desert and oceanic aerosol over Solar Village, there are a total 274 days of AOT and AWE data in 2005, in which AWE changes from −0.003 to 1.276 and the mean AWE is 0.519. There are 14 days under below 0.062 AOT (670 nm) conditions. When using radiation measurements from those 14 days, and inputting an AWE of 1.0 into the calibrations, a below 0.5% uncertainty is estimated according to Fig. 6. Therefore, a below 2% uncertainty, caused by assuming an AWE of 1.0 and an AII of 0.01, can be achieved for a wide variety of aerosol types when radiation measurements under below 0.062 AOT (670 nm) conditions are used in the calibrations. The calibration accuracy should be improved further by using AWE and AII values that are close to their real values for a given aerosol type.

4. Summary

A new method has been proposed to simultaneously calibrate GSI, DSI, and SSI measurements. The method directly takes the WRR as the calibration standard and uses on-site radiation measurements as inputs. Two simple but effective techniques are used to achieve this goal. The first is to scale the SSI and GSI detection sensitivities under overcast skies, which is based on the fact that SSI should be equal to GSI when DSI is completely scattered and absorbed. The second is to retrieve the AOT under clear yet relatively clean conditions from R_f derived from β_R. Thereafter, the retrieved AOTs are used to drive an RTM to calculate atmospheric transmittance and thereby to calibrate solar radiometers. The method was applied to calibrate radiation measurements at Xianghe. The calibration robustness was validated based on comparisons of two kinds of AOT retrievals with AERONET AOT products. The first was AOT retrievals from R_f, and the second was BEM AOT retrievals from original and recalibrated HDSI. The major results can be summarized as follows.

The calibration uncertainties of DSI, GSI, and SSI were estimated to be within −4.0% to 2.9%, −5.9% to 2.4%, and −6.1% to 4.9%, respectively. The estimations were basically coincident with 3%, 6%, and 6% uncertainties (DSI, GSI, and SSI) (Stoffel 2005).

The maximum deviation of AOT retrievals based on R_f from AERONET AOT is 0.026 and the standard deviation was 0.008, indicating a very good agreement. A good agreement between BEM AOTs from both original and recalibrated HDSI and AERONET AOT

was also obtained. More importantly, the application of recalibrated HDSI data in the BEM AOT retrievals resulted in lower deviation from AERONET AOT, as compared to the original HDSI data.

The calibration transfer coefficients for the GSI, DSI, and SSI in summer are larger than those in winter, which is likely caused by lower instrument sensitivity when the temperature is high. The temperature effect will be further investigated in future work.

Sensitivity analysis showed the calibration uncertainty to be below 2% for suburban aerosol over the Xianghe site if there were $\pm 0.5/\pm 0.005$ deviations in AWE/AII. The smaller the AOT was, the weaker the effect of AWE and AII uncertainty on the calibration. A below -2% uncertainty, caused by assuming an AWE of 1.0 and AII of 0.01, can be achieved for a wide variety of aerosol types when radiation measurements under below 0.062 AOT (670 nm) conditions are used in calibrations. Furthermore, a better calibration accuracy should be obtained if the AWE and AII inputs are even closer to their real values for a given aerosol type. How to select more suitable AWE and AII values in calibrations remains a problem to be further studied in future work.

The outstanding feature of this method is that prior calibrations of DSI, GSI, and SSI measurements are not required. Furthermore, AOT, the most important factor determining the atmospheric transmittance under clear and clean conditions, is retrieved from the pyranometer measurements. Therefore, the method can potentially be used to calibrate historical pyranometer measurements if water vapor content is available. The unique advantage of this method also lies in that it can be used to correct historic radiation measurements and monitor radiometer performance. It is especially suitable in cases with more clear days and smaller AOT. We intend to use the method to recalibrate DSI, GSI, and SSI measurements from Chinese meteorological observatories since 1960, and then retrieve AOTs from the recalibrated radiation data. The effects of input parameter uncertainties will also be further investigated.

Acknowledgments. This research was supported by the National Basic Research Program (Grant 2011CB403401), the National Natural Science Foundation of China (Grants 41175029 and 41175031), and the Strategic Priority Research Program of the Chinese Academy of Sciences (XDA05100300). Maintenance of the solar radiometers by Mr. Weidong Nan and other staff members at the Xianghe Observatory is greatly appreciated. Special appreciation is also extended to the NASA AERONET group for processing the AERONET data.

REFERENCES

Coulson, K. L., 1975: *Solar and Terrestrial Radiation: Methods and Measurements.* Academic Press, 322 pp.

Dubovik, O., and M. King, 2000: A flexible inversion algorithm for retrieval of aerosol optical properties from sun and sky radiance measurements. *J. Geophys. Res.,* **105,** 20 673–20 696, doi:10.1029/2000JD900282.

——, B. N. Holben, T. F. Eck, A. Smirnov, Y. J. Kaufman, M. D. King, D. Tanre, and I. Slutsker, 2002: Variability of absorption and optical properties of key aerosol types observed in worldwide locations. *J. Atmos. Sci.,* **59,** 590–608, doi:10.1175/1520-0469(2002)059<0590:VOAAOP>2.0.CO;2.

Dutton, E., J. J. Michalsky, T. Stoffel, B. W. Forgan, J. Hickey, D. W. Nelson, T. L. Alberta, and I. Reda, 2001: Measurement of broadband diffuse solar irradiance using current commercial instrumentation with a correction for thermal offset errors. *J. Atmos. Oceanic Technol.,* **18,** 297–314, doi:10.1175/1520-0426(2001)018<0297:MOBDSI>2.0.CO;2.

Eck, T. F., B. N. Holben, J. S. Reid, O. Dubovik, A. Smirnov, N. T. O'Neill, I. Slutsker, and S. Kinne, 1999: Wavelength dependence of the optical depth of biomass burning, urban, and desert dust aerosols. *J. Geophys. Res.,* **104,** 31 333–31 349, doi:10.1029/1999JD900923.

——, and Coauthors, 2005: Columnar aerosol optical properties of AERONET sites in central eastern Asia and aerosol transport to the tropical mid-Pacific. *J. Geophys. Res.,* **110,** D06202, doi:10.1029/2004JD005274.

Gilgen, H., and A. Ohmura, 1999: The global energy balance archive. *Bull. Amer. Meteor. Soc.,* **80,** 831–850, doi:10.1175/1520-0477(1999)080<0831:TGEBA>2.0.CO;2.

Holben, B. N., and Coauthors, 1998: AERONET—A federated instrument network and data archive for aerosol characterization. *Remote Sens. Environ.,* **66,** 1–16, doi:10.1016/S0034-4257(98)00031-5.

Ji, Q., and S.-C. Tsay, 2010: A novel nonintrusive method to resolve the thermal dome effect of pyranometers: Instrumentation and observational basis. *J. Geophys. Res.,* **115,** D00K21, doi:10.1029/2009JD013483.

——, ——, K. M. Lau, R. A. Hansell, J. J. Butler, and J. W. Cooper, 2011: A novel nonintrusive method to resolve the thermal dome effect of pyranometers: Radiometric calibration and implications. *J. Geophys. Res.,* **116,** D24105, doi:10.1029/2011JD016466.

Ohmura, A., and Coauthors, 1998: Baseline Surface Radiation Network (BSRN/WCRP): New precision radiometry for climate research. *Bull. Amer. Meteor. Soc.,* **79,** 2115–2136, doi:10.1175/1520-0477(1998)079<2115:BSRNBW>2.0.CO;2.

Qiu, J., 1998: A method to determine atmospheric aerosol optical depth using total direct solar radiation. *J. Atmos. Sci.,* **55,** 744–758, doi:10.1175/1520-0469(1998)055<0744:AMTDAA>2.0.CO;2.

——, 2001: Broadband extinction method to determine atmospheric aerosol optical properties. *Tellus,* **53B,** 72–82, doi:10.1034/j.1600-0889.2001.01064.x.

——, 2003: Broadband extinction method to determine aerosol optical depth from accumulated solar direct radiation. *J. Appl. Meteor.,* **42,** 1611–1623, doi:10.1175/1520-0450(2003)042<1611:BEMTDA>2.0.CO;2.

——, X. Xu, and J. Yang, 2008: Accuracy estimations of global solar irradiance measurements at seven meteorological observatories of Beijing. *J. Appl. Meteor. Sci.,* **19,** 287–295.

Roosen, R. G., R. J. Angione, and C. H. Klemeke, 1973: Worldwide variations in atmospheric transmission: Baseline

results from Smithsonian observations. *Bull. Amer. Meteor. Soc.,* **54,** 307–316, doi:10.1175/1520-0477(1973)054<0307:WVIATB>2.0.CO;2.

Schaaf, C. B., and Coauthors, 2002: First operational BRDF, albedo nadir reflectance products from MODIS. *Remote Sens. Environ.,* **83,** 135–148, doi:10.1016/S0034-4257(02)00091-3.

Smirnov, A., B. Holben, T. Eck, O. Dubovik, and I. Slutsker, 2000: Cloud screening and quality control algorithms for the AERONET database. *Remote Sens. Environ.,* **73,** 337–349, doi:10.1016/S0034-4257(00)00109-7.

Stamnes, K., S.-C. Tsay, W. J. Wiscombe, and K. Jayaweera, 1988: Numerically stable algorithm for discrete-ordinate-method radiative transfer in multiple scattering and emitting layered media. *Appl. Opt.,* **27,** 2502–2509, doi:10.1364/AO.27.002502.

Stoffel, T., 2005: Solar infrared radiation station handbook. ARM Tech. Rep. ARM-TR-025, National Renewable Energy Laboratory, 29 pp.

Stothers, R. B., 1996: Major optical thickness perturbations to the stratosphere from volcanic eruptions: Pyrheliometric period, 1881-1960. *J. Geophys. Res.,* **101,** 3901–3920, doi:10.1029/95JD03237.

WMO, 1982: Abridged final report of the eighth session. WMO Series, No. 590, Commission for Instruments and Methods of Observation, World Meteorological Organization, 89 pp.

Xia, X., H. Chen, P. Wang, W. Zhang, P. Goloub, B. Chatenet, T. F. Eck, and B. N. Holben, 2006: Variation of column-integrated aerosol properties in a Chinese urban region. *J. Geophys. Res.,* **111,** D06204, doi:10.1029/2005JD006203.

——, Z. Li, P. Wang, H. Chen, and M. Cribb, 2007: Estimation of aerosol effects on surface irradiance based on measurements and radiative transfer model simulations in northern China. *J. Geophys. Res.,* **112,** D22S10, doi:10.1029/2006JD008337.

Yang, J., and J. Qiu, 2002: A method for estimating precipitable water and effective water vapor content from ground humidity parameters. *Chin. J. Atmos. Sci.,* **26,** 81–96.